

Major Activity of NewSUBARU

1. Photonuclear reaction of iodine-129 with laser-Compton scattering γ -ray

The photonuclear reaction cross section of iodine-129 was measured using a polarized laser-Compton scattering γ -ray beam in an energy range from 13.9 to 19.7 MeV. The maximum cross section was evaluated to be $220 \text{ mb} \pm 50\%$ at a photon energy of $15.9 \text{ MeV} \pm 4\%$. We did not observe any appreciable difference in the cross sections for linearly and circularly polarized γ -ray beams, within the limits of experimental error.

Figure 2 shows photonuclear reaction cross section σ_R derived by assuming the value of σ_s proposed by Berger *et al.* [1] in an energy range from 13.9 to 19.7 MeV for both linear (crossed) and circular (circled) polarizations of incident γ -rays. The γ -ray photon energy was scanned by changing the energy of the electron beam from 890 to 1060 MeV. The probability distribution of the signal intensity against the count rate was assumed to be a Poisson distribution. From the standard deviation, the error bars in Fig. 2 were calculated to be 12% at respective γ -ray energy. The error in the absolute value of the cross section was evaluated to be $\pm 50\%$ by taking into account the errors due to the alignment accuracy between the γ -ray beam and the target axes; this accuracy was a major factor compared with the errors in the number of iodine-129 atoms ($< \pm 1\%$), the flux of the γ -rays ($\pm 2\%$), their energy spread (-3%), and the peak detection efficiency of the Ge detector ($\pm 10\%$).

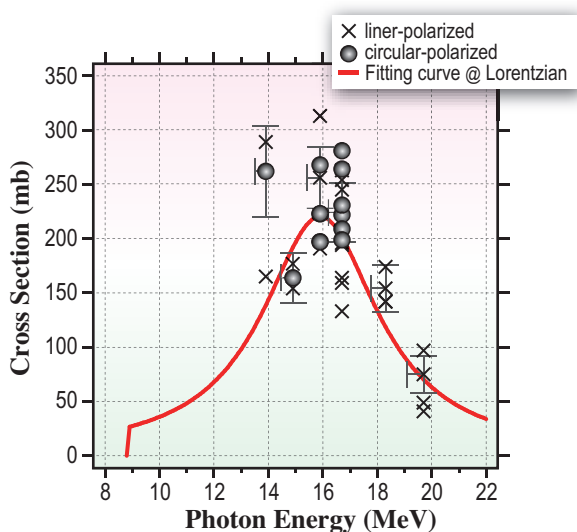


Fig. 2. Dependence of photonuclear reaction cross section of iodine-129 on energy and polarization of γ -ray photons.

2. EUV interference lithography

EUV interference lithographic system that can evaluate the resists for half pitch (hp) 22 nm, hp 16 nm, and hp 11 nm nodes has been developed. Since a replicated resist pattern with high accuracy and high resolution can be obtained by EUV interference lithography using light diffraction and interference, the resolution and line edge roughness (LER) of resist itself can be evaluated without other factors. This EUV-IL exposure system is installed at beamline BL9. Since the 10.8-m-long undulator (LU) is employed as a light source, spatial coherence is large and a fine pattern can be replicated over the entire exposure area. Up to now, a 60-nm-pitch transmission grating pattern, which corresponds to hp 15 nm resist pattern on a wafer, has been fabricated.

The intensity of the light produced from the LU is 1,000 times higher than that from the bending magnet. In addition, a highly coherent light is produced from the LU. By Young's interference experiment, it was confirmed that the spatial coherence length is longer than 1 mm. EUV-IL two window transmission gratings were used. When the EUV light is irradiated to one grating window, the light diffracts into 0th, -1 st, and $+1$ st orders. With two window gratings, -1 st-order light from one window grating and $+1$ st-order light from another window grating interfere to produce the interference fringes on a wafer. Consequently, a resist pattern with a half the pitch size of the transparent grating is replicated on the wafer. The transmission grating is fabricated at the EUVL R&D center. Figure 3 shows the replicated resist pattern of the commercial resist ZEP-520A for electrons utilizing EUV-IL. SEM photographs of hp 22.5 nm, hp 20 nm, and hp 15 nm resist patterns are shown in this figure. We obtained resist patterns with high contrast.

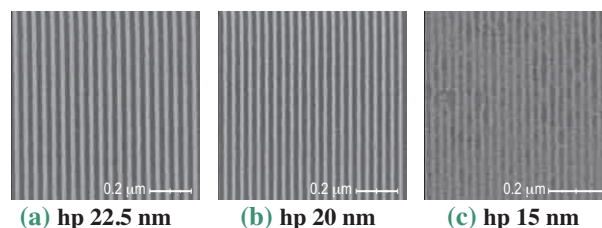


Fig. 3. Exposure results obtained by EUV-IL.

3. High-sensitivity detection of Polychlorinated Biphenyl on three-dimensional lab-on-a-CD

This presents high-sensitivity detection of polychlorinated biphenyl (PCB) in a three-dimensional lab-on-a-CD, which consists of multiple disks with three-dimensional microchannel networks. To perform the automatic sequencing of the competitive protocol, capillary-barrier-type passive valves with vertically embedded capillary valves were designed and fabricated. We successfully demonstrated the detection of polychlorinated biphenyl.

Figure 4 shows the photographs of planar microchannel disks of polydimethylsiloxane (PDMS) and through-hole poly(methyl methacrylate) (PMMA) disks fabricated by standard rapid prototyping and deep X-ray lithography. A bundle-like capillary structure of square capillaries (75 μm in diameter) are formed on the PMMA disks for the effective immobilization of antibody. To demonstrate the detection of PCB, the bundle-like capillary structure is immobilized with anti-PCB antibody and blocked with BSA by off-chip immobilization. Then the disk is reversibly bonded with PDMS (also blocked) to construct the 3D lab-on-a-CD. We observed a strong effect of the micromachining accuracy of the bundle-like capillary structure on the reproducibility of the assay.

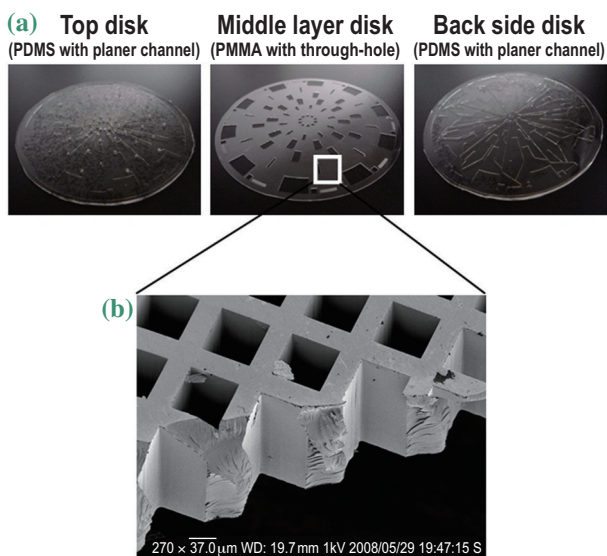


Fig. 4. (a) Photographs of fabricated disks of 3D lab-on-a-CD. (b) SEM image of bundle-like capillary structure for antibody immobilization.

4. Present Status of Material Analysis Beamline at BL5 for Industrial Enterprises

A material analysis beamline for industrial enterprises' use was completed at BL5 in March 2008. BL5 consists of two branch lines: a double-crystal monochromator beamline (BL5A) for use in the higher-energy region (1300-4000 eV) and a varied-line-spacing plane grating (VLSPG) monochromator beamline (BL5B) for use in the lower-energy region (50-1300 eV). These two branch lines can be operated simultaneously. The entire range of useful energy of the BL5 is the soft X-ray region from 50 to 4000 eV. The X-ray absorption fine structure (XAFS) measurements of the total electron yield (TEY) and fluorescence yield (FLY) can be performed at BL5A and BL5B. In addition, the X-ray photoelectron spectra (XPS) can be measured at BL5B.

We readjusted of the optical mirror and measured standard samples by the TEY method in BL5B. Figure 5 shows the near-edge X-ray absorption fine structure (NEXAFS) spectra of calcium fluoride (CaF_2) powder obtained using a grating with 400 lines/mm and calcium $L_{3,2}$ -edge. The spectra were normalized to I_0 and the linear pre-edge background was removed. After optical adjustment (slit width: 50 μm), the improvement of resolution was verified by comparison with that before optical adjustment (slit width: 200 μm). The calcium $L_{3,2}$ -edge spectral shape of CaF_2 almost corresponds to the spectrum reported by Naftel *et al.* [2].

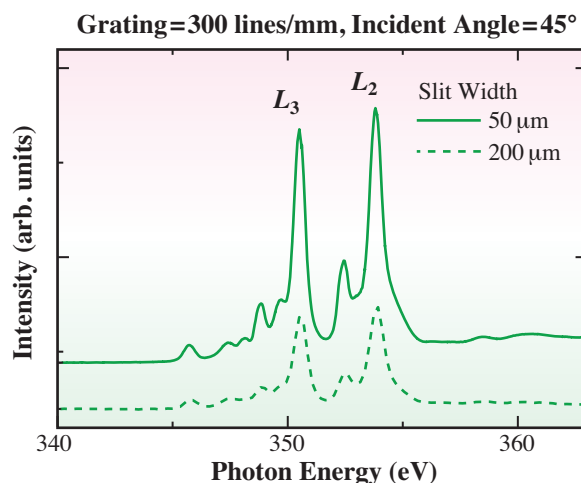


Fig. 5. CaF_2 Ca $L_{3,2}$ -edge NEXAFS spectra.

References

- [1] M.J. Berger *et al.*: "XCOM: Photon Cross Sections Database," <<http://www.nist.gov/pml/data/xcom/index.cfm>>
- [2] S.J. Naftel *et al.*: J. Synchrotron Rad. **8** (2001) 255.